Clay Minerals, (2016) **51**, 635–651

Occurrence of tosudite in the Guezouman, Tarat and Tchirezrine 2 formations, hosts of uranium deposits in Niger (Tim Mersoï basin)

SOPHIE BILLON[1,2,*,†], PATRICIA PATRIER[2], DANIEL BEAUFORT[2], PAUL SARDINI[2] AND AURÉLIA WATTINNE-MORICE[3]

[1] *Société ERM, rue Michel Brunet, Bat. 35, 86000 Poitiers, France*
[2] *Université de Poitiers, UMR 7285 CNRS, IC2MP, rue Michel Brunet, Bat. 35, 86073 Poitiers cedex 9, France*
[3] *AREVA, 1 place Jean Millier, 92084 Paris la Défense, France*

(*Received 1 November 2015; revised 27 May 2016; Guest Editor: Atsuyuki Inoue*)

ABSTRACT: Tosudite, a regularly interstratified chlorite-smectite, crystallizes as an alteration mineral of several preexisting Al-bearing silicates (feldspars, kaolin minerals, chlorites) present in arkosic sandstones hosted in uranium deposits in Niger. X-ray diffraction patterns show a sharp superstructure at 29–29.6 Å for an air-dried state and a peak at 30.8–31.6 Å following ethylene glycol solvation. The 060 reflection at 1.507–1.509 Å indicates an overall dioctahedral character, and the very low coefficient of variation of the d_{001} reflections for the solvated mineral (0.03–0.13) permits validation of the regular interstratification justifying its identification as tosudite. Microprobe analysis allowed specification of the component layers of this mixed-layer mineral. The chlorite is a di-trioctahedral type analogous to sudoite ($Si_3Al_4Mg_2(OH)_8$), and the smectite component is a low-charge montmorillonite type ($Si_4Al_{1.67}Mg_{0.33}M^+_{0.33}(OH)_4$). Tosudite is characterized by large Al_2O_3 and MgO contents and small Fe content; its composition corresponds approximately to the formula $((Si_7Al)O_{20}(Al_{4.5}Mg_{2.3}Fe^{3+}_{0.2})M^+_{0.3}(OH)_{10})$, where octahedral occupancy is ~7. Scanning electron microscope (SEM) observations show that tosudite is closely associated with some uranium minerals: tosudite crystallization occurred during a late alteration event which post-dates burial diagenesis and during which uranium was remobilized by Mg-rich oxidizing fluids.

KEYWORDS: tosudite, uranium deposits, Niger, sandstones, oxidizing fluids, post-diagenetic alteration.

Although it has been known for a long time, tosudite is not a common clay mineral in natural systems (Frank-Kamenetskii *et al*., 1965). Tosudite has been the subject of relatively few studies compared to other interstratified clay minerals presenting the same type of mixed-layered structure (such as corrensite). According to the recommendations of the Nomenclature Committee of the International Association for the study of clays (AIPEA) (Bailey, 1982), the name tosudite is valid for 1:1 regular interstratification of chlorite and smectite that is dioctahedral on average. According to the nomenclature, this specification allows several combinations of layers among which only interstratification of di-dioctahedral chlorite with either dioctahedral or trioctahedral smectites and interstratification of di-trioctahedral chlorite with dioctahedral smectites have been documented. According to the literature, tosudite has been determined primarily in hydrothermally altered felsic rocks (*e.g.* Sudo & Kodama, 1957; Shimoda, 1969; Brown *et al*., 1974; Bartier *et al*., 2008) in which the two interstratified layer components tend to be

*E-mail: sophie.billon@univ-poitiers.fr
†This work was originally presented during the session 'The many faces of chlorite', part of the Euroclay 2015 conference held in July 2015 in Edinburgh, UK.
DOI: 10.1180/claymin.2016.051.4.07

essentially dioctahedral and can often incorporate significant amounts of Li in their structure (Creach *et al*., 1986; Merceron *et al*., 1988). However, there is also evidence that tosudite can form during the diagenesis of siliciclastic sediments (Wilson, 1971; Morrison & Parry, 1986; Daniels & Altaner, 1990; Garvie, 1992; Harrison *et al*., 2004; Hillier *et al*., 2006) and also possibly during more severe thermobarometric conditions corresponding to the transition between diagenesis and very low-grade metamorphism (Cruz & Andreo, 1996). Even if the thermal conditions of its formation are poorly constrained, tosudite is considered to form in a wide temperature range varying between 100° and >300°C according to the geological setting (Beaufort *et al*., 2015 and references therein).

The purpose of the present study was to document a new occurrence of tosudite in sandstone formations of the Tim Mersoï sub-basin (Niger), which hosts several uranium deposits of economic interest (Forbes, 1989; Pagel *et al*., 2005). The main goals were: (1) to examine the petrographic relationships between tosudite and authigenic minerals including uranium-bearing minerals; (2) to determine both crystal structure and chemical composition of nearly pure specimens to determine carefully the nature of the interstratified layers that make up this mineral; and (3) to discuss the conditions of formation and the possible origin of tosudite in such a geological system.

GEOLOGICAL SETTING AND PREVIOUS WORK ON BASIN EVOLUTION AT THE REGIONAL SCALE

The Tim Mersoï basin, a sub-basin of the Iullemmeden basin, hosts several uranium deposits that have been discovered successively since 1958 (Pagel *et al*., 2005). Most of these uranium deposits are located in the eastern part of the Tim Mersoï basin, near the major regional N–S fault of Arlit-In-Azawa (AIA) and to the west of the Aïr mountains (Fig. 1).

The sedimentary series of the Tim Mersoï basin, which range from Carboniferous (Terada series) to Cretaceous (Irhazer series) (Fig. 2), have been described by Valsardieu (1971), Sempéré (1981), Pacquet (1969) and Gerbeaud (2006).

The Tagora unit consists of four fluvial sandstone formations: the Guezouman, Tarat, Madaouela and Arlit formations. The Guezouman and Tarat formations are separated by the thin Tchinezogue formation formed during a marine transgression event. Both the Guezouman and Tarat formations host uranium deposits which are exploited by the COMINAK and SOMAIR mining companies, respectively, in the Arlit area (Figs 1, 2). Samples from the Tamgak prospect (SOMAÏR mining site) show that both the Guezouman and Tarat formations originated in a sedimentary environment particularly suited to the precipitation of uranium mineralization (mostly observed as pitchblende): organic matter is abundant and sandstones are very permeable (Billon *et al*., 2009).

The Izegouandan and Agades series, which are of Permian and Jurassic age, respectively, correspond to red detrital deposits of the Tim Mersoï basin. These red series derived from alteration products generated by a hot climate with seasonal variations (wet and dry) and are attributed to a fluvial and lacustrine environment. The Tchirezrine 2 formation (Agades series), consisting mainly of sandstones, hosts the Imouraren deposit, located 80 km south of the Arlit area (Figs 1, 2). The Jurassic formation of Tchirezrine 2 is also very porous, but differs from the Carboniferous formations of Guezouman and Tarat, because no reducing agents such as organic matter were observed. Uraniferous mineralization consists mainly of hexavalent uranium-bearing minerals (Billon, 2014).

Sandstone petrography

Most of the sandstones from both the Carboniferous and Jurassic formations investigated in this study show a detrital mineralogy dominated by monocrystalline quartz as well as variable amounts of different types of alkali feldspars (albite, orthoclase and microcline) and minor amounts of polycrystalline quartz. Accessory minerals are scarce and consist mainly of white micas, zircon, apatite and monazite.

The sandstones studied appear very heterogeneous in terms of sorting (poorly to well sorted) and grain size (fine- to coarse-grained). Despite the fact that the shape of detrital grains has been modified by compaction, brittle deformation and dissolution, the initial morphology of detrital quartz and feldspars seems to have been variable (sub-rounded to sub-angular). The amount of clay matrix is also highly variable, ranging from <3% to >35% according to normative calculation based on whole-rock chemistry and X ray diffraction (XRD) analyses.

The overall colour of Carboniferous and Jurassic sandstones differs according to their mineralogical contents: (1) Tarat and Guezouman reduced sandstones, which contain organic matter and pyrite, display a dark grey to greenish colour; and (2) Tchirezrine 2 oxidized sandstones, which contain

https://doi.org/10.1180/claymin.2016.051.4.07 Published online by Cambridge University Press

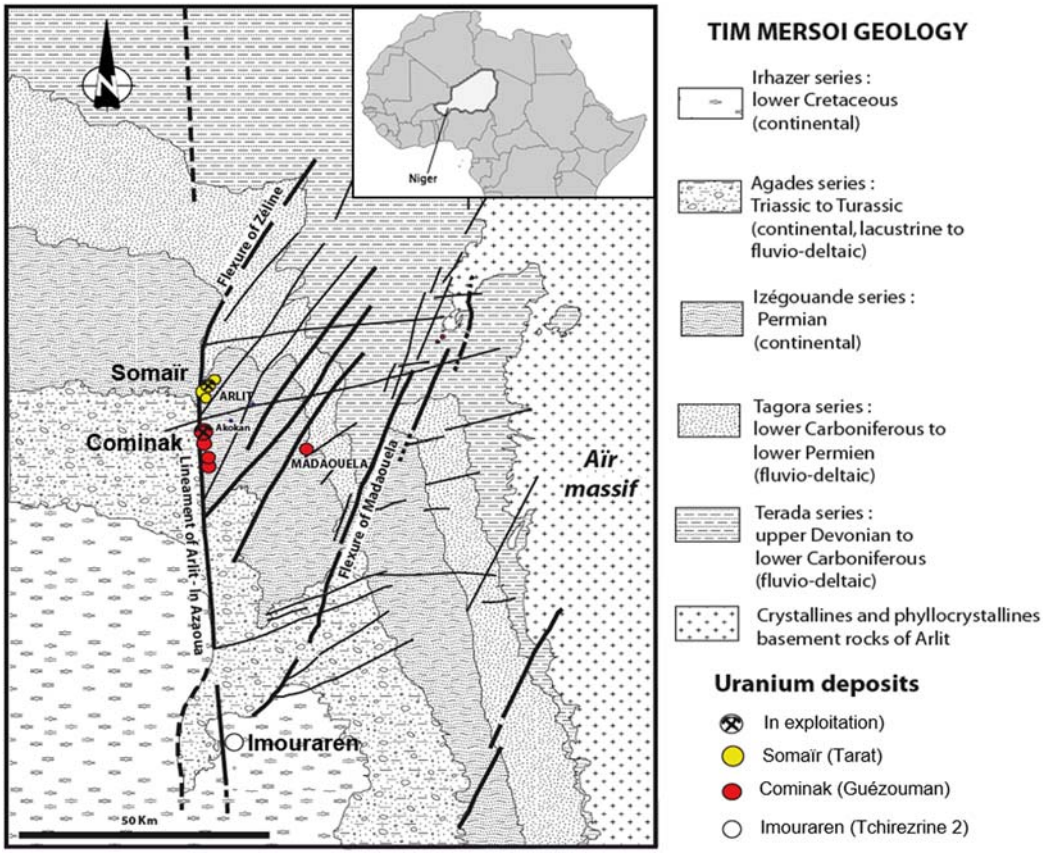

FIG. 1. Location of the Tim Mersoï basin and of the Arlit and Imouraren areas (modified from Cavellec, 2006).

disseminated hematite and no organic matter, display mainly a typical reddish colour.

For both Carboniferous and Jurassic sandstones, the mineralogical and textural modifications related to burial diagenesis were followed by brittle deformation events (fracturation).

Burial diagenesis

Diagenetic processes related to burial of siliciclastic sediments have been observed in all of the samples studied. Compaction is evidenced by the presence of concavo-convex mutual quartz grain contacts (with local features of stylolitic surfaces) and by micro-fractures in detrital feldspars close to point contacts. Pressure solution and related syncompactional authigenic quartz overgrowths are common and especially abundant in the clay-poor samples. Note that compactional features are very scarce in the Carboniferous samples affected by early dolomite cementation.

Two main types of authigenic clay minerals were formed during the burial history of sandstones: (1) coarse-grained minerals of the kaolin sub-group; and (2) fine-grained Fe-rich chlorite. In the Carboniferous samples, kaolin minerals predominate over chlorite, whereas it is the opposite in the Jurassic samples. The crystal habits of the kaolin minerals range from a vermicular arrangement of pseudohexagonal plates typical of kaolinite to a blocky habit typical of dickite (Fig. 3a,b). According to XRD patterns, dickite is scarcer in the Jurassic formation than in the Carboniferous ones. Nevertheless, the relative intensities of $d_{20\bar{2}}$, $_{1\bar{3}1}$ reflections of kaolinite and $d_{132,\ 20\bar{4}}$ reflections of dickite demonstrate that kaolinite also predominates over dickite in both Jurassic and Carboniferous samples. In conditions of normal geothermal gradient, the predominance of kaolinite

https://doi.org/10.1180/claymin.2016.051.4.07 Published online by Cambridge University Press

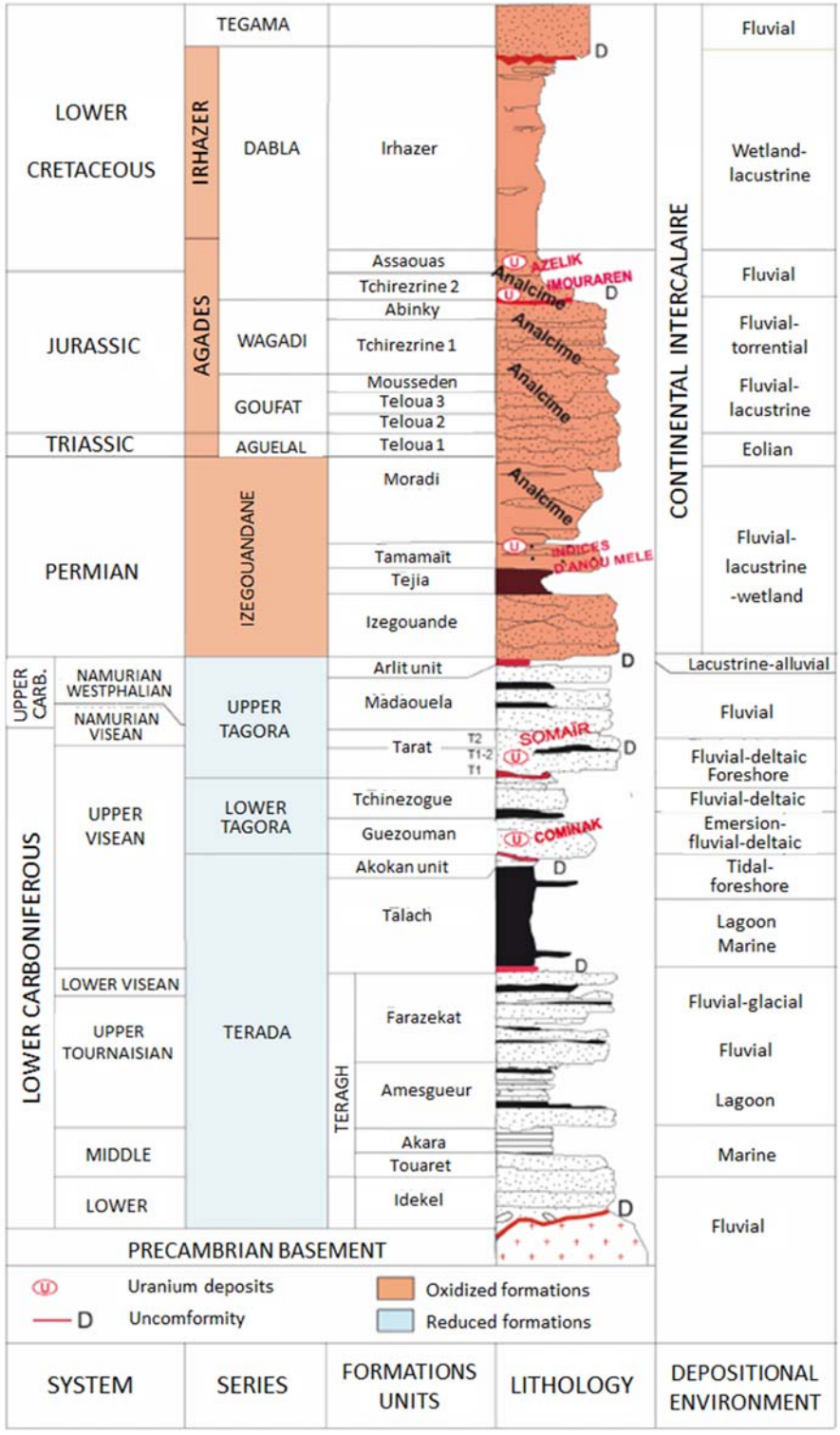

FIG. 2. Lithostratigraphy of the Tim Mersoï basin (modified from Coquel *et al*., 1995).

https://doi.org/10.1180/claymin.2016.051.4.07 Published online by Cambridge University Press

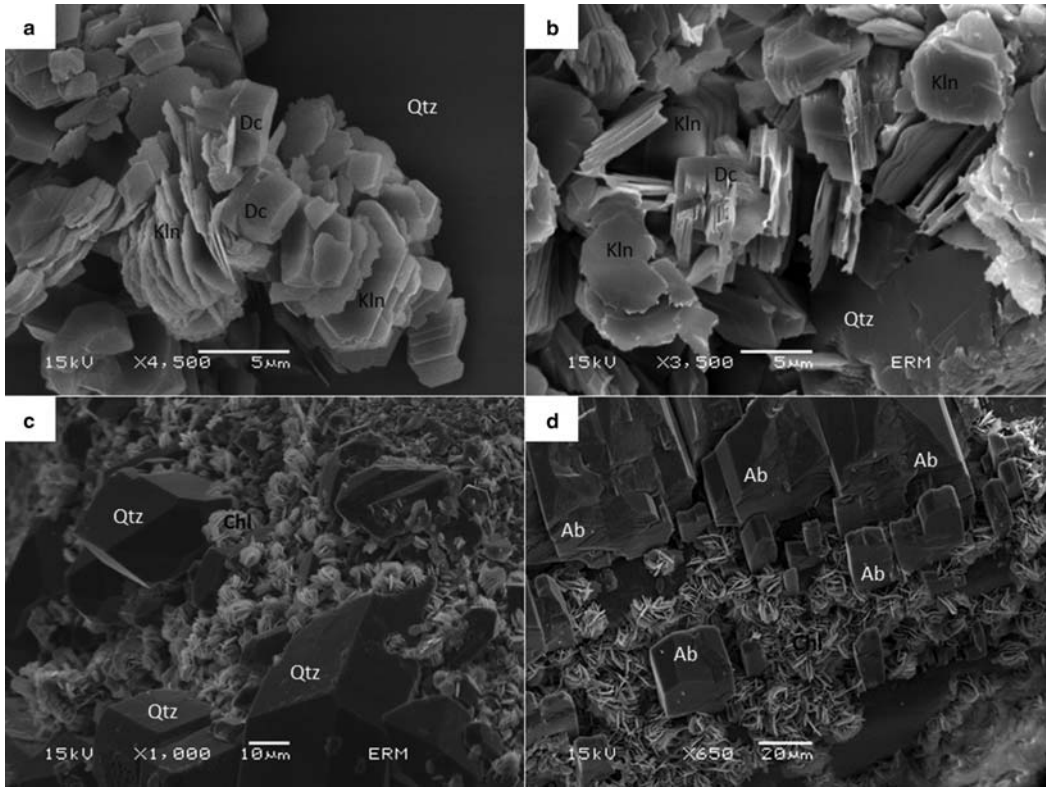

FIG. 3. Textural aspects of authigenic clay minerals formed during burial diagenesis of the sandstones (SEM images). (a,b) Mixture of pseudohexagonal plates of kaolinite (Kln) (partially dissolved) and blocky crystals of dickite (Dc) in Carboniferous sandstones (a) and Jurassic sandstones (b), respectively. (c) Discontinuous coating of detrital quartz grains by Fe-rich chlorite spherules (Chl) and authigenic quartz overgrowths (Qtz) in Carboniferous sandstones. (d) Discontinuous coating of detrital albite grains by Fe-rich chlorite spherules (Chl) and authigenic albite overgrowths (Ab) in Jurassic sandstones.

over dickite in these sandstones is indicative of maximum burial depth which did not exceed 3–3.5 km (Beaufort *et al.*, 1998; Lanson *et al.*, 2002).

Fe-rich chlorite occurs essentially as a discontinuous coating on detrital quartz and feldspars, partially inhibiting overgrowths of quartz and albite (Fig. 3c, d). This mineral shows euhedral platy crystals that are oriented perpendicular to the framework grain surface arranged in either a rosette or spherule-like structure. Microprobe and XRD data of this chlorite are similar to those of Fe-rich chlorite commonly reported at low temperatures in siliciclastic reservoir sandstones (*i.e.* chlorite interstratified with small amounts of berthierine-like layers and Ib $\beta = 90°$ polytype) (Beaufort *et al*, 2015 and references therein).

Petrographic observations indicate that both kaolin minerals and Fe-rich chlorite crystallized at an early stage during the burial history. Chlorite coatings tend to inhibit the development of quartz overgrowth and features of mutual stopping between authigenic kaolinite and quartz overgrowth were commonly observed. No clear paragenetic relationship between authigenic kaolin minerals and chlorite can be deduced from petrographic observations.

In Jurassic sandstones, three other authigenic minerals are observed: (1) analcime formed earlier from destabilization of volcanic materials; the latter are no longer scan today because they have been dissolved completely (Pacquet, 1969); (2) albite overgrowths, which are synchronous with quartz overgrowths; and (3) scarce illite, related to the incipient illitization of the pore-filling diagenetic kaolinite. The abundant presence of analcime and albite (Na-rich silicates) indicates that diagenetic fluids in the Jurassic formation were

https://doi.org/10.1180/claymin.2016.051.4.07 Published online by Cambridge University Press

probably more alkaline than those occurring in Carboniferous formations where authigenic analcime and albite are absent.

The paragenetic sequence observed in the Carboniferous and Jurassic sandstones is summarized in Fig. 4.

Brittle deformation events

These events resulted in the development of a microfracture network in the sandstones. Brittle deformation is observed along micro-fault planes and, in particular, affects the detrital feldspars, which were broken into fragments, further separated during the deformation, leading locally to a cataclastic fine-grained matrix. Observations made on thin sections indicate that brittle deformation post-dates the authigenic minerals related to the burial diagenesis.

SAMPLES AND METHODS

Approximately 40 samples of Carboniferous sandstones (Guezouman and Tarat formations) were collected from five drill-holes located in the Tamgak prospect (Arlit area), and 240 samples of Jurassic sandstones (Tchirezrine 2 formation) were taken from 26 drill-holes spread across the Imouraren deposit. Most of the Carboniferous and Jurassic samples were fine- to coarse-grained sandstones investigated according to the following analytical methods. Note that Carboniferous and Jurassic samples were not always analysed using the same equipment because the two sets of samples come from different studies.

X-ray diffraction (XRD)

Acquisitions of XRD patterns for the Carboniferous samples were performed with a Panalytical X'pert Pro diffractometer (PANalytical B.V., Almelo, The Netherlands), and XRD patterns for the Jurassic samples were obtained using a Bruker D8 Advance diffractometer. These two diffractometers have a Bragg-Brentano θ/2θ configuration, using a copper source with wavelength for $K\alpha_1$ of 1.540598 Å, 40 kV and 40 mA current.

Oriented clay mounts (<10 μm fraction separated by sedimentation) were prepared by filter peel (pore diameter of 0.8 μm), a method that produces mounts that have reasonable crystallite orientation (Bish & Reynolds, 1989). Oriented mounts were analysed in the air-dried state (AD) at room humidity and after solvation with liquid ethylene glycol (EG). The XRD patterns were obtained using diffraction data that were recorded in scanning mode and converted to step patterns (with a step size of 0.01°2θ using a 1 s counting time per step). Diffraction data were recorded from 2.5 to 30°2θ for the oriented mounts and from 2 to 65°2θ for randomly oriented powders of tosudite.

Petrographic data (including morphology and textural relationships) were recorded from polished thin sections, previously coated by carbon, using a Nikon ECLIPSE E600 POL polarizing optical microscope

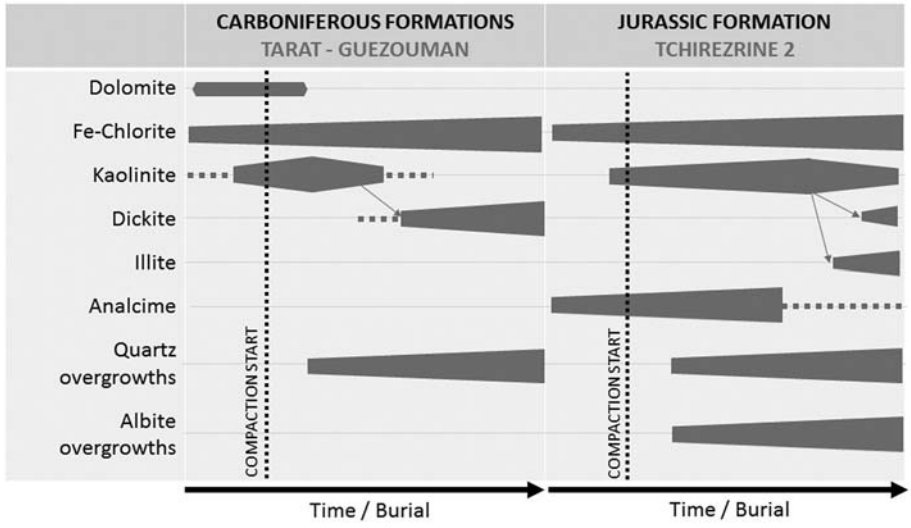

FIG. 4. Relative chronology of diagenetic mineral paragenesis in the Carboniferous and Jurassic sandstones.

https://doi.org/10.1180/claymin.2016.051.4.07 Published online by Cambridge University Press

and from the examination of rock slabs, previously coated with gold, using a JEOL 5600LV scanning electron microscope (SEM).

Chemical analyses

Minerals observed in thin sections of the Carboniferous samples were analysed using a CAMECA SX50 microprobe using a wavelength-dispersive spectrometer (WDS). The analysed elements were Na, Mg, Al, Si, K, Ca, Ti, Mn and Fe. The microprobe was calibrated using synthetic and natural oxides and silicates ($MnTiO_3$, hematite, albite, orthoclase and diopside) and corrections were made using a CAMECA PAP matrix. The analytical conditions were as follows: current intensity of 4 nA; accelerating voltage of 15 kV; spot size of 2 μm; and counting time of 10 s per element. The relative error was <1.5%. Total Fe was considered arbitrarily as ferrous or ferric according to the nature of the mineral analysed.

Around 50 thin sections of the Jurassic samples were analysed using the SEM equipped with an energy dispersive X-ray analyser (EDS, silicon drift detector). The analytical conditions were as follows: acceleration voltage 15 kV, probe current 1 nA, working distance 16.5 mm, and counting time 100 s. The standards used for EDS consist of albite (Na, Al, Si), almandine (Mg, Fe), diopside (Ca), orthoclase (K), spessartine (Mn) and Ti metal (Ti).

RESULTS

Late alteration and tosudite occurrence

Late alteration, which occurred after burial diagenesis and brittle deformation, was related to a strong dissolution of most of the aforementioned Al-bearing detrital and diagenetic minerals followed by their replacement by a pore-filling tosudite (in both Carboniferous and Jurassic sandstones) and occasionally by the association of montmorillonite and hematite (exclusively in Jurassic sandstones) (Billon *et al*., 2013). The spatial distribution of the tosudite matrix is highly heterogeneous, but it is more abundant in the sandstones that show evidence of micro-fracturing and the presence of disseminated hematite. The latter observation suggests that tosudite formation was controlled at least partially by fractures which promoted solute transport of oxidizing solutions, the origin and timing of which still remain unclear. Occasional pore cementation by late calcite into Carboniferous sandstones was also related to this alteration event. In Jurassic sandstones, late harmotome (Ba-zeolite: $(Ba_{0.5}Ca_{0.5}KNa)_5(Al_5Si_{11}O_{32})12H_2O$) and calcite are often observed as filling vertical joints.

Observations by SEM indicate that tosudite shows a boxwork pattern with flakes oriented perpendicular to the surface of the detrital grains on which tosudite crystallizes (Fig. 5a,b). At higher magnification, the boxwork appears to be composed of thin, folded packets of anhedral platy crystals, the average size of which can reach up to 5 μm. Such a morphological characteristic is very similar to those reported previously for corrensite (Hillier, 1994; Beaufort *et al*., 1997) or sudoite (Billault *et al*., 2002). Petrographic observations indicate that tosudite post-dates all the other silicate minerals of the sandstones. It seems to have crystallized in the alteration sites of all pre-existing Al-bearing silicates. The replacement of dissolved detrital feldspars (orthoclase, microcline and albite) by tosudite is often observed in strongly altered samples. Indeed, fractured and dissolved K-feldspars show a significant tosudite coating (Fig. 5c,d).

More or less pervasive occurrences of tosudite were also observed in the diagenetic clay matrix; chlorite and kaolinite were strongly dissolved in tosudite-rich sandstones. The frequent observation of kaolinite grains embedded in the tosudite matrix indicates that tosudite post-dated and replaced kaolinite in Carboniferous sandstones (Fig. 6a,b). Fe-rich diagenetic chlorite is strongly dissolved in both Carboniferous and Jurassic sandstones and relics of this mineral are also embedded in the boxwork pattern of the tosudite matrix (Fig. 6d,e). In case of incipient alteration, Fe-rich chlorite spherules display a very particular morphology that consists of individual chlorite plates forming the spherules, coated and bridged by very thin films of tosudite (Fig. 6c). In Jurassic sandstones, a low-charge montmorillonite associated with hematite occurred as a replacement of dissolved Fe-rich diagenetic chlorite.

Petrographic evidence of relationships between tosudite and uranium minerals

Coexisting tosudite and uraniferous minerals have been observed in several places in both Carboniferous and Jurassic sandstones. However, significant differences have been noted according to the redox conditions of the Carboniferous and Jurassic formations.

In the reduced sandstones of the Carboniferous formations (Tarat and Guezouman), aggregates of tiny globular pitchblende (UO_2) that contain uranium as U^{4+} have been observed in the alteration sites where altered

https://doi.org/10.1180/claymin.2016.051.4.07 Published online by Cambridge University Press

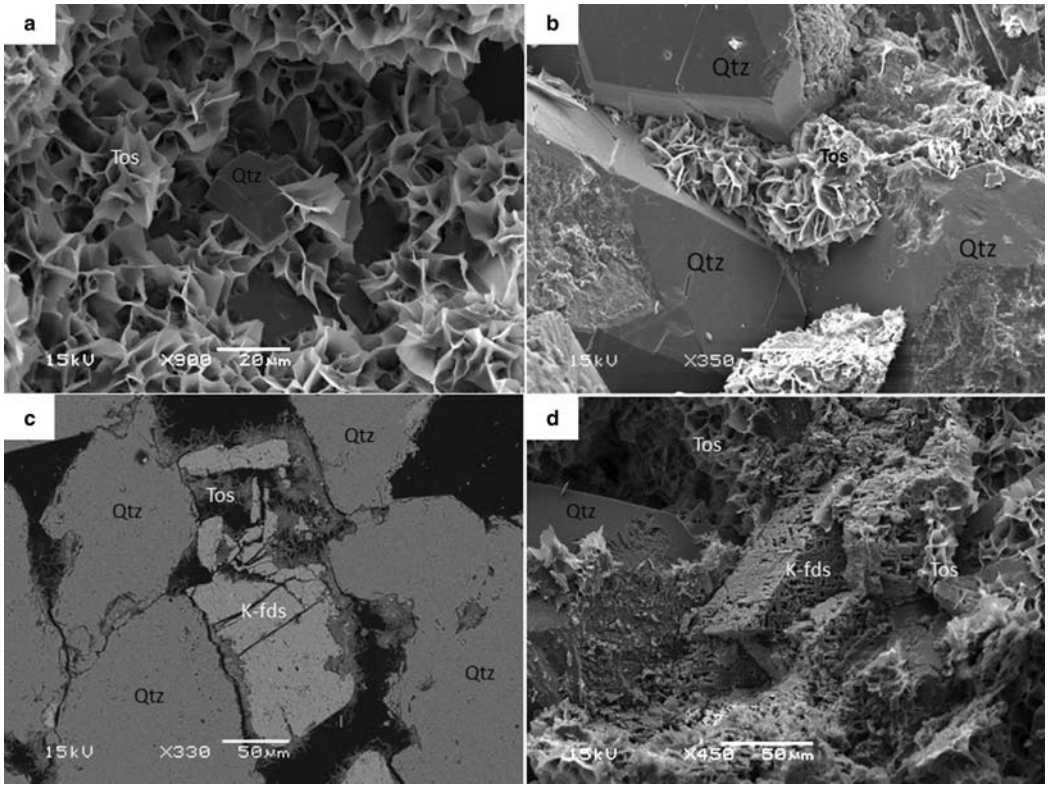

FIG. 5. Morphological characteristics of tosudite and its relationships with K-feldspars in the sandstone samples (SEM images). (a,b) Honeycomb morphology of tosudite (Tos) in Carboniferous sandstones (a) and Jurassic sandstones (b), respectively. (c) Tosudite (Tos) crystallized on a coating of fractured K-feldspar (K-fds) in Carboniferous sandstones. (d) Tosudite (Tos) crystallized on a coating of dissolved K-feldspar (K-fds) in Jurassic sandstones.

Fe-chlorite is partially replaced by tosudite. Such pitchblende blebs crystallized either as a continuous layer at the boundary between the Fe-chlorite and replacing tosudite matrix (Fig. 7a) or as a nearly continuous coating on the Fe-chlorite plates encountered next to the 'tosudite front' (Fig. 7b).

In the oxidized sandstones of the Jurassic formation (Tchirezrine 2), tosudite is frequently associated with two uraniferous minerals that contain U essentially as U^{6+}: metatyuyamunite ($((CaUO_2)_2V_2O_8 3H_2O)$) and uranophane ($Ca(UO_2)_2(SiO_3OH)_2 5H_2O$) (Fig. 7c). Tosudite is also associated with hematite (Fig. 7d). Hematite occurs more often with montmorillonite, both replacing Fe-chlorite.

Mineralogical data for tosudite

The XRD patterns of the clay concentrates from sandstones affected by late alteration processes are typical of those of a regularly ordered chlorite-smectite mixed-layer mineral with sharp superstructure reflections at 29–29.6 Å (AD) and 30.8–31.6 Å (EG) and with up to ten higher orders in the 2–30°2θ Cu-*K*α range (Figs 8a, 9a). The sharpness of these reflections is characteristic of rather thick crystallites and is consistent with the relatively large size of the phyllosilicate flakes observed using SEM (Fig. 5a,b). The other X-ray reflections observed in these patterns correspond to small amounts of kaolinite, quartz and feldspars for the Carboniferous samples and to Fe-chlorite, analcime, quartz and feldspars for the Jurassic sandstones.

The 060 reflection at 1.507 Å (Fig. 8b) and at 1.509 Å (Fig. 9b), coupled with chemical analyses (octahedral occupancies close to 7 atoms per $O_{20}(OH)_{10}$), suggest that such a mixed-layer mineral, which is dioctahedral on average, includes a di-trioctahedral component in its structure. The

https://doi.org/10.1180/claymin.2016.051.4.07 Published online by Cambridge University Press

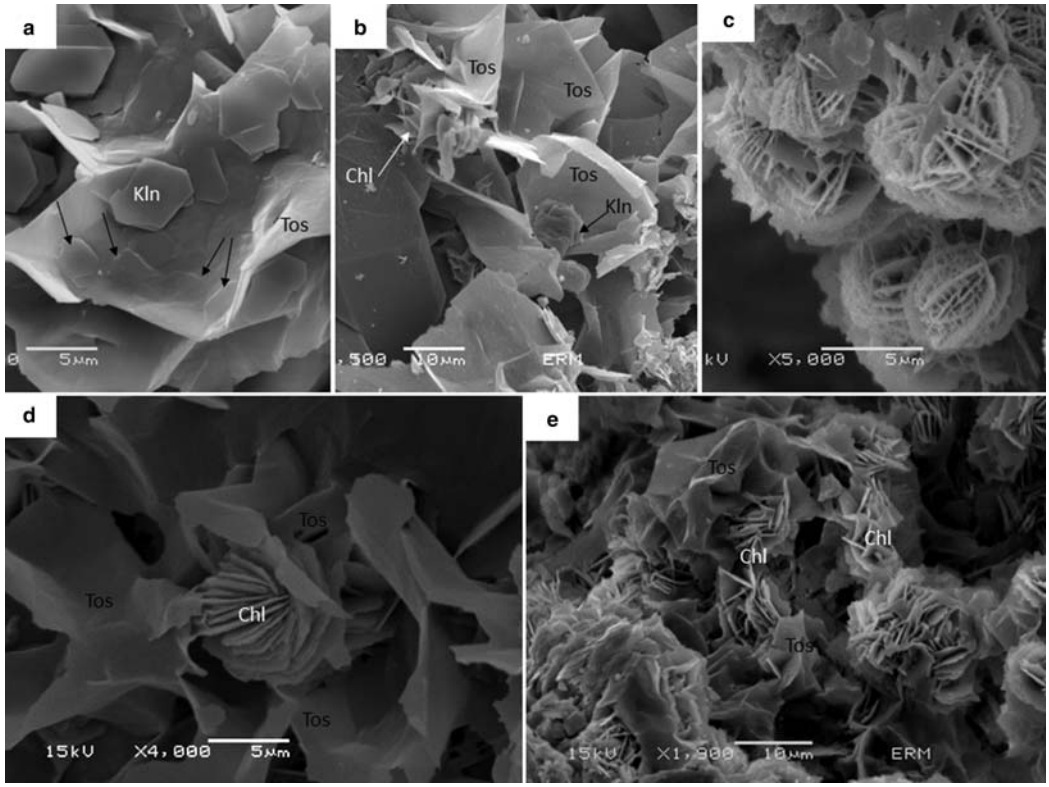

FIG. 6. Relationships between tosudite and other clay minerals in the sandstone samples (SEM images): (a) kaolinite (kln and black arrows) embedded in tosudite (Tos) in Carboniferous sandstones; (b) relics of dissolved chlorite (Chl) and kaolinite (Kln) in tosudite (Tos) in Jurassic sandstones; (c) incipient replacement of chlorite spherules by thin films of tosudite; (d,e) replacement of Fe-rich chlorite (Chl) presenting a spherulitic texture by tosudite (Tos) in Carboniferous sandstone (d) and Jurassic sandstone (e), respectively.

coefficient of variation of the d_{001} reflections (CV) was calculated from the series of basal XRD reflections of EG-saturated oriented preparations. According to the recommendation of Bailey (1982), the CV should be <0.75 for regular interstratifications. In this study, the CV is very small (0.03–0.13) and permits the name tosudite to be used for this mineral, which is a regularly ordered 50:50 mixed-layer chlorite-smectite (Brown *et al*., 1974; Pablo-Galan & Chavez-Garcia, 1994; Nishiyama *et al*., 1975).

Tosudite mineral chemistry

Concerning Carboniferous samples, ~100 microprobe analyses were performed on thin sections of the alteration sites in which the tosudite matrix is widespread. Only 30 chemical analyses were performed on tosudite from Jurassic sandstones using EDS.

Chemical composition and calculated structural formulae (on the basis of 25 oxygens) of eight representative analyses are reported in Table 1 (five for tosudite from the Carboniferous formation, three for tosudite from the Jurassic formation). Tosudite of both Carboniferous and Jurassic sandstones is characterized by large Al_2O_3 and MgO contents, small Fe content (<2.5% of Fe_2O_3) and relatively small total wt. % values (81–85%), attributable to the OH content of the mineral and the porous state of the clay matrix. However, tosudite from the Jurassic formation is slightly poorer in MgO and richer in Al_2O_3 and Fe_2O_3 than tosudite from Carboniferous sandstones.

Calculated on the basis of 25 oxygens, all the structural formulae (Table 1) are consistent with a chlorite-smectite mixed layer containing equal amounts of di-trioctahedral chlorite and low-charge dioctahedral smectite (*i.e.* octahedral occupancy close

https://doi.org/10.1180/claymin.2016.051.4.07 Published online by Cambridge University Press

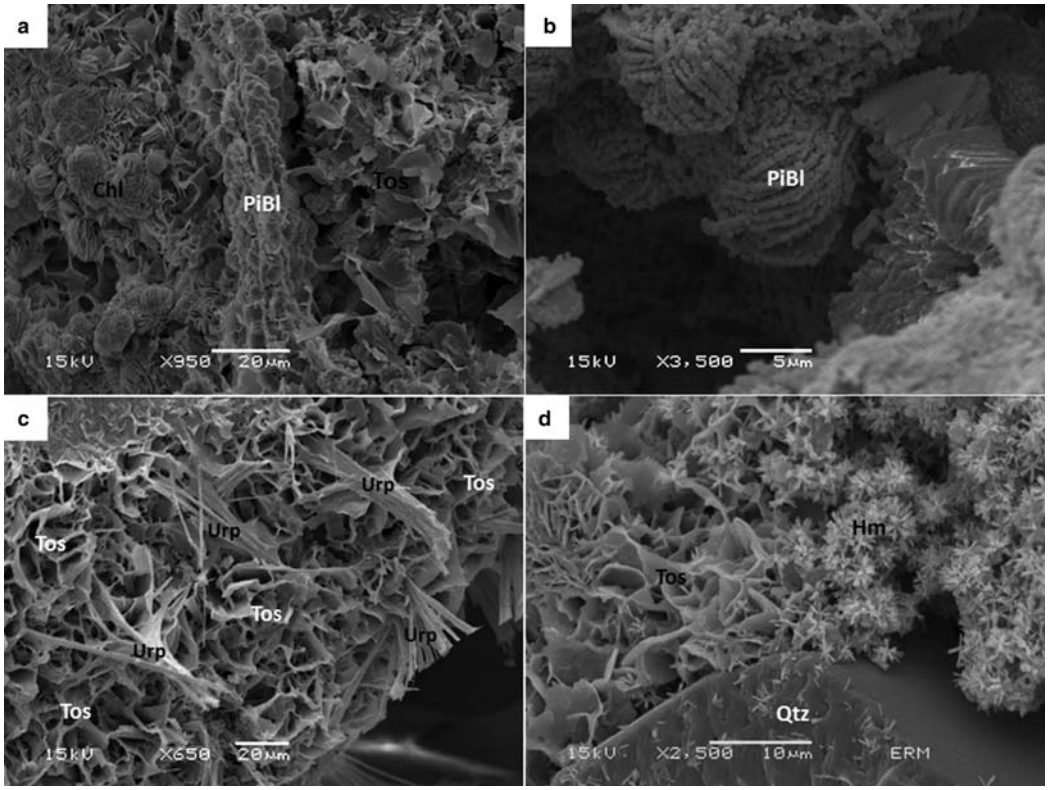

FIG. 7. Uraniferous mineralization associated with tosudite (SEM images). (a) Alteration front of Fe-rich chlorite (Chl) and its replacement by tosudite (Tos) in Carboniferous sandstones. Note the occurrence of a continuous layer of pitchblende (PiBl) at the boundary between the Fe-chlorite and the replacing matrix of tosudite. (b) Fe-rich chlorite spherules coated by very fine blebs of pitchblende (PiBl) close to the sites in which tosudite replaces chlorite in Carboniferous sandstones. (c) Association of tosudite (Tos) and uranophane (Urp) in Jurassic sandstones. (d) Association of tosudite (Tos) and dendritic habit of hematite (Hm) in Jurassic sandstones.

to 7 atoms and interlayer charge near 0.44 per $O_{20}(OH)_{10}$ formula unit). The projection of all the microprobe analyses of tosudite from Carboniferous and Jurassic formations in the chemographic representation MR3-2R3-3R2 (Velde, 1985) shows a whole compositional field of the 'tosudite' clay matrix. The field is spread between sudoite and low-charge montmorillonite end-members, with a maximum number of point analyses that fall at mid-distance between these two end-members (Fig. 10).

The Al- and Mg-rich character of the chlorite component and its very low Fe content are indeed consistent with that of a theoretical Mg-sudoite ($Si_3Al_4Mg_2O_{10}(OH)_8$). Conversely, a simple subtraction of the theoretical composition of sudoite from the structural formulae obtained in Table 1 confirms that the dioctahedral smectite component is consistent with montmorillonite (Table 2). Even if such a calculation remains an approximation because of the assumptions of an equal number of smectite and chlorite components and the use of a theoretical composition for sudoite, it is interesting to note that the analyses in Table 2 are centred around values close to that of a theoretical montmorillonite (*i.e.* very small negative charge in the tetrahedral sheet). Natural sudoite frequently deviates from the theoretical composition by minor Fe for Al and/or Mg substitutions (up to 0.5 Fe atoms per formula unit) (Billault *et al.*, 2002 and references therein), which would explain negative values for Mg for tosudite from the Jurassic formation (Table 2).

Note that some individual analyses of tosudite from the Carboniferous formation are closer to the sudoite end-member, whereas certain Jurassic sandstones are

https://doi.org/10.1180/claymin.2016.051.4.07 Published online by Cambridge University Press

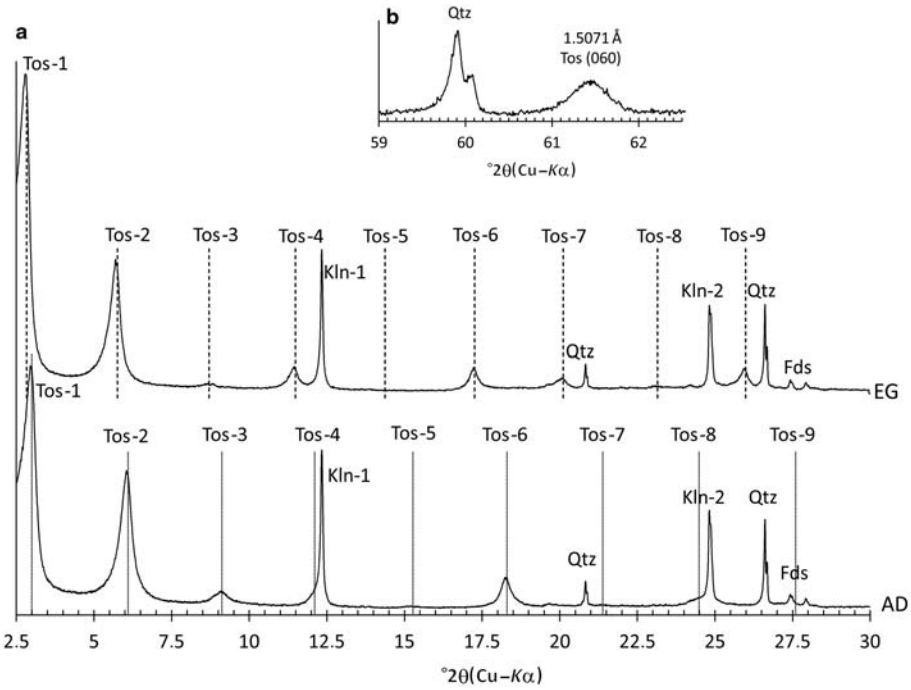

FIG. 8. XRD patterns of tosudite in Carboniferous sandstones: (a) XRD patterns of oriented preparation in the air-dried state (AD) and in the glycol-saturated state (EG). Tos, tosudite; Kln, kaolinite; Qtz, quartz; Fds, feldspars. The number after the mineral-name abbreviation corresponds to the order of 00l peaks. (b) XRD patterns of 060 reflection of randomly oriented preparations. Tos, tosudite; Qtz, quartz.

closer to the montmorillonite end-member (Fig. 10). For analyses of tosudite from Jurassic sandstones, this observation could be explained by the co-occurrence of montmorillonite that replaced dissolved Fe-rich chlorite.

DISCUSSION

This study of sandstone samples from the Tarat, Guezouman and Tchirezrine 2 formations has demonstrated that tosudite is the dominant clay mineral formed during a late alteration event that post-dated both burial diagenesis and subsequent brittle deformation of the Carboniferous to Jurassic sandstone formations surrounding the Arlit fault. Investigations by XRD and microprobe indicate that even if this mixed-layer mineral is dioctahedral on average, it is Al,Mg-rich and consists of the interstratification of layers of a di-trioctahedral chlorite with a composition equivalent to sudoite and a dioctahedral smectite that is equivalent to montmorillonite. Even if tosudite has not been reported explicitly in the sandstone formations of the Tim Mersoï basin, several occurrences of mixed-layer clay minerals presenting XRD patterns and Al Mg-rich chemical compositions similar to those of tosudite have been reported in previous works on other deposits of the Arlit area (Paquet, 1968; Forbes, 1989; Cavellec, 2006) as mixed-layer chlorite-smectite, corrensite or dioctahedral corrensite. This suggests that tosudite could have a regional extension in the Carboniferous to Jurassic clastic sedimentary rocks that host the uranium deposits of Niger. Tosudite is related to an alteration process which post-dated the burial diagenesis of the basin, the physical-chemical conditions of which are poorly constrained.

In this respect, two main types of geological environments have been reported for the natural occurrence of tosudite: (1) areas that experienced hydrothermal activity related to circulation of acidic solutions at temperatures generally >200°C (Shimoda, 1969; Brown *et al*., 1974; Nishiyama *et al*., 1975; Creach *et al*., 1986; Merceron *et al*., 1988; Daniels & Altaner, 1990; Pablo-Galan & Chavez-Garcia, 1994; Hillier *et al*., 1996; Harrison *et al*., 2004); and (2) areas

https://doi.org/10.1180/claymin.2016.051.4.07 Published online by Cambridge University Press

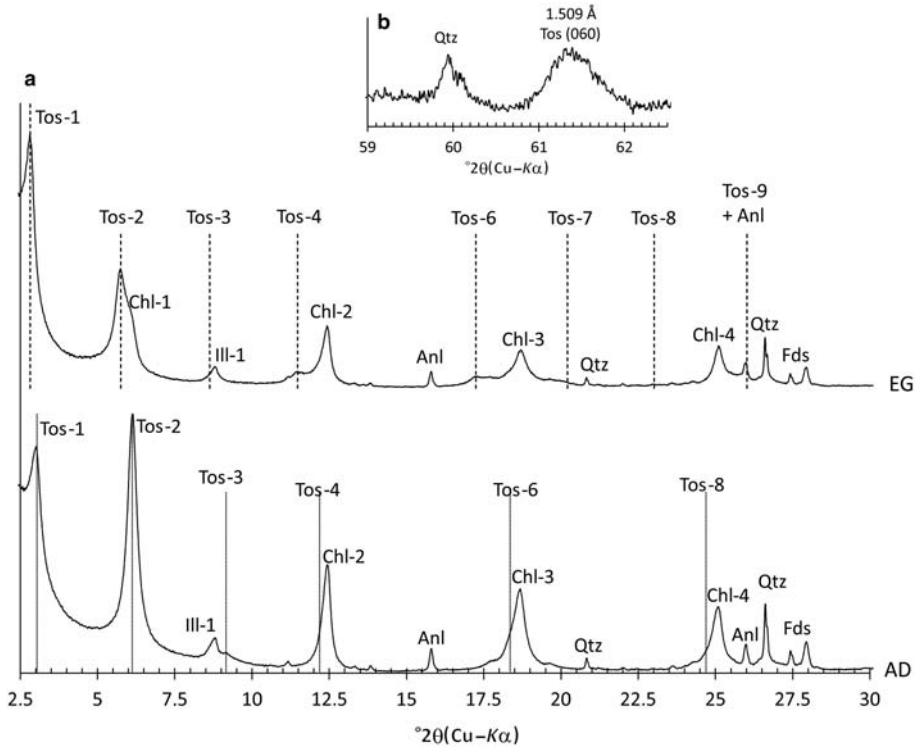

FIG. 9. XRD patterns of tosudite in Jurassic sandstones: (a) XRD patterns of oriented preparations in the air-dried state (AD) and in the ethylene glycol-saturated state (EG). Tos, tosudite; Ill, illite; Chl, chlorite; Anl, analcime; Qtz, quartz; Fds, feldspars. The number after the mineral-name abbreviation corresponds to the 00l peaks. (b) XRD patterns of 060 reflection of randomly oriented preparations. Tos, tosudite; Qtz, quartz. Chlorite identified with tosudite in this sample is considered as trioctahedral considering the 060 reflection (close to 1.539 Å) and because of the relative intensity of 00l peaks (the 003 reflection has greater intensity than the 002 reflection for sudoite).

that have undergone burial diagenesis of clastic sedimentary formations that are thought to have been an important pathway for circulation of fluids with rather high ionic strength (Kulke, 1969; Wilson, 1971; Morrison & Parry, 1986; Garvie, 1992; Hillier *et al*., 2006), at lower temperatures (between 100 and 200°C).

In the Carboniferous formation of Guezouman and Tarat, tosudite occurred in permeable sandstones that contain intrinsic reducing agents (carbonaceous matter) and also host several uranium deposits. As the deposition or the remobilization of uranium in sandstones depends essentially on the existence (and eventually the migration) of redox fronts permitting either the precipitation of uranium by reduction of U^{6+} (highly soluble) to U^{4+} (highly insoluble) or the remobilization of the previously mineralized uranium by oxidizing solutions, it seems that the change in redox conditions, which controlled the uranium migration-deposition processes, could also have played a significant role in the crystallization of tosudite encountered near these two types of uranium deposits. Indeed, the alteration petrography and the crystal chemistry of tosudite presented in this study argue for a relationship between tosudite, hematite and the uranium minerals identified in the sandstone formations of the Tim Mersoï sub-basin. In reduced Carboniferous sandstones that have been altered only slightly, pitchblende occurs along the replacement fronts of diagenetic Fe-rich chlorite by tosudite. In oxidized Jurassic sandstones, U^{6+}-bearing minerals (metatyuyamunite and uranophane) coexist with abundant tosudite, montmorillonite and hematite. These occurrences suggest that tosudite, hematite and U-minerals crystallized at the same time. As such, tosudite could be an interesting marker of uranium migration during the basin's geological history (Fig. 11).

https://doi.org/10.1180/claymin.2016.051.4.07 Published online by Cambridge University Press

TABLE 1. Representative WDS (Carboniferous sandstones) and EDS (Jurassic sandstones) analyses and structural formulae of tosudite.

	Carboniferous				Jurassic			
	1	2	3	4	5	6	7	8
SiO_2	43.32	40.81	43.93	43.68	43.88	39.91	41.64	42.70
Al_2O_3	28.43	27.82	28.43	26.62	28.75	29.67	31.45	31.75
MgO	9.96	10.61	9.59	9.86	10.56	7.85	7.78	7.92
Fe_2O_3	1.48	1.24	1.45	1.69	1.21	2.32	2.06	2.01
TiO_2	0.11	0.00	0.00	0.21	0.00	0.08	0.00	0.00
MnO	0.03	0.13	0.14	0.14	0.07	0.01	0.04	0.00
CaO	0.75	0.69	0.84	0.72	0.74	0.43	0.55	0.58
Na_2O	0.10	0.12	0.12	0.20	0.16	0.15	0.12	0.13
K_2O	0.17	0.28	0.57	0.15	0.27	0.45	0.60	0.65
Sum	84.18	81.41	84.49	83.11	85.36	80.87	84.24	85.74
Numbers of cations on the basis of $O_{20}(OH)_{10}$								
Si	7.00	6.84	7.06	7.16	6.99	6.80	6.80	6.84
Al^{IV}	1.00	1.16	0.94	0.84	1.01	1.20	1.20	1.16
Al^{VI}	4.42	4.34	4.45	4.30	4.39	4.76	4.85	4.84
Mg	2.40	2.65	2.30	2.41	2.51	1.99	1.89	1.89
Fe^{3+}	0.18	0.16	0.18	0.21	0.14	0.30	0.25	0.24
Ti	0.01	0.00	0.00	0.03	0.00	0.01	0.00	0.00
Mn	0.00	0.02	0.02	0.02	0.01	0.00	0.01	0.00
Oct.	7.02	7.16	6.94	6.97	7.06	7.06	7.00	6.97
Ca	0.13	0.12	0.14	0.13	0.13	0.08	0.10	0.10
Na	0.03	0.04	0.04	0.06	0.05	0.05	0.04	0.04
K	0.04	0.06	0.12	0.03	0.06	0.10	0.12	0.13
Int ch.	0.33	0.34	0.44	0.35	0.36	0.31	0.36	0.37

All Fe has been arbitrarily considered as Fe^{3+}. Oct., octahedral occupancy; Int. ch., interlayer charge.

Tosudite (referred to as dioctahedral corrensite) has also been reported in the Permian red beds of Lisbon Valley (Paradox basin, Utah, USA), which hosts uranium deposits (Morrison & Parry, 1986). In addition to the close similarity between the mineralogical properties of tosudite from the Lisbon Valley and tosudite from Niger, it appears that there are also similarities between their potential links with uranium deposition. In the Permian red beds from Lisbon Valley, tosudite crystallized in bleached, permeable sandstones that also contain the uranium ore and many traces of contrasting redox palaeoconditions.

Another argument supporting the cogenetic formation of tosudite and uraniferous minerals in both Carboniferous and Jurassic formations, can be found in the crystal-chemistry of tosudite, which strongly suggests that this mineral crystallized under rather oxidizing conditions.

Dissolution of ferrous phyllosilicates such as diagenetic Fe-rich chlorite (XFe > 0.7) and their replacement by tosudite (XFe < 0.1) and hematite is geochemical evidence for leaching of Fe from the silicate minerals during the alteration process. Such leaching can be explained by the oxidation of ferrous iron during the interaction of of Fe-bearing diagenetic minerals (chlorite and sulfides) with oxidizing (and U-bearing) solutions infiltrated along a late fracture network. As incorporation of ferric iron in phyllosilicates such as chlorite, di-tri- or trioctahedral, is very limited (Beaufort *et al.*, 1992; Nelson & Guggenheim 1993; Billault *et al.* 2002), most of the ferric iron released in solution precipitated as cogenetic hematite.

Such a geochemical process has been described for the replacement of metamorphic chlorite by sudoite and hematite in the mineralized zones of the Kiggavik uranium deposit (Riegler *et al.*, 2014).

Several authors have tried to determine the origin of and the thermal conditions at which diagenetic tosudite forms in sedimentary basins (see reviews in Beaufort

https://doi.org/10.1180/claymin.2016.051.4.07 Published online by Cambridge University Press

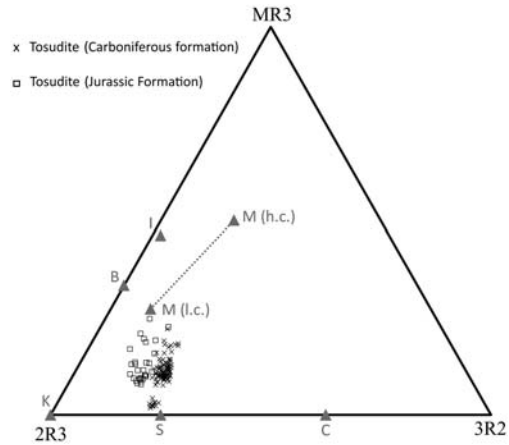

FIG. 10. Representation of WDS (for Carboniferous sandstones) and EDS (for Jurassic sandstones) analyses of tosudite in the triangular diagram MR3-3R2-2R3 (Velde, 1985). Grey triangles represent pure phases: C, chamosite $(Si_3Al)O_{10}$ $(Fe^{2+}_5Al)(OH)_8$ or/and clinochlore $(Si_3Al)O_{10}(Mg_5Al)(OH)_8$; S, sudoite $(Si_3Al)O_{10}(Mg_2Al_3)(OH)_8$; M (h.c.), high-charge montmorillonite $Si_4O_{10}(Mg_{0.6}Al_{1.4})(OH)_2K_{0.6}$; M (l.c.), low-charge montmorillonite $Si_4O_{10}(Mg_{0.3}Al_{1.7})(OH)_2K_{0.3}$; I, illite $(Si_{3.3}Al_{0.7})O_{10}(Mg_{0.1}Al_{1.9})(OH)_2$ $K_{0.8;}$ B, beidellite $(Si_{3.5}Al_{0.5})O_{10}Al_2(OH)_2K_{0.5}$; K, kaolinite $Si_2Al_2O_5(OH)_4$.

et al., 2015 and references therein). According to them, tosudite would belong to a conversion series of dioctahedral smectite-to-sudoite (Morrison & Parry, 1986) or kaolinite-to-sudoite (Hillier *et al*., 2006), which progresses with increasing burial and temperature in the presence of Mg-rich saline solutions. In the Tim Mersoï basin, petrographic observations indicate that tosudite did not result from a unique mineral reaction. It crystallized as a replacing mineral after dissolution of most of the Al-bearing detrital and diagenetic minerals (*i.e.* feldspars, kaolin minerals and chlorite). This fact indicates that tosudite from the uranium deposits of the Tim Mersoï basin is not a product of a specific diagenetic conversion series but the product of a strong alteration process of the Al-rich silicates in response to important infiltration of oxidizing solutions in the permeable sandstones. Pagel *et al*. (2005) suggested that important circulation of hot, deep fluids could have been drained by the Arlit fault system. Cavellec (2006) proposed the possibility of hydrothermal circulations in the vicinity of the Arlit fault. In the present state, nothing constrains precisely the alteration stage at which tosudite is associated with such fluid types is not constrained precisely. More detail of the spatial distribution of tosudite at a regional scale is needed to test its potential link with the Arlit fault history. Furthermore, the substantial deviation of the composition of diagenetic Fe-rich chlorite towards both tosudite and sudoite end-members (Fig. 12), evidenced by a compilation of chlorite compositions from the Arlit area and the Imouraren area (Forbes, 1989; Cavellec, 2006; Billon *et al*., 2009; Patrier *et al*., 2009; Rigault, 2010), suggests that tosudite could be mixed with diagenetic

TABLE 2. Hypothetical structural formulae of dioctahedral smectite estimated from the assumption of equal amounts of smectite and di-trioctahedral chlorite components in the mixed-layer mineral and a theoretical formula of sudoite as $Si_3Al_4Mg_2O_{10}(OH)_8$.

	Carboniferous				Jurassic			
	1	2	3	4	5	6	7	8
Si	4.00	3.84	4.06	4.16	3.99	3.80	3.80	3.84
Al	1.42	1.50	1.39	1.14	1.40	1.96	2.05	2.00
Mg	0.40	0.65	0.30	0.41	0.51	−0.01	−0.11	−0.11
Fe^{3+}	0.18	0.16	0.18	0.21	0.14	0.30	0.25	0.24
Ti	0.01	0.00	0.00	0.03	0.00	0.01	0.00	0.00
Mn	0.00	0.02	0.02	0.02	0.01	0.00	0.01	0.00
Oct	2.01	2.33	1.89	1.81	2.06	2.26	2.20	2.13
Ca	0.13	0.12	0.14	0.13	0.13	0.08	0.10	0.10
Na	0.03	0.04	0.04	0.06	0.05	0.05	0.04	0.04
K	0.04	0.06	0.12	0.03	0.06	0.10	0.12	0.13
Int ch.	0.33	0.34	0.44	0.35	0.36	0.31	0.36	0.37

Int. ch., interlayer charge.

https://doi.org/10.1180/claymin.2016.051.4.07 Published online by Cambridge University Press

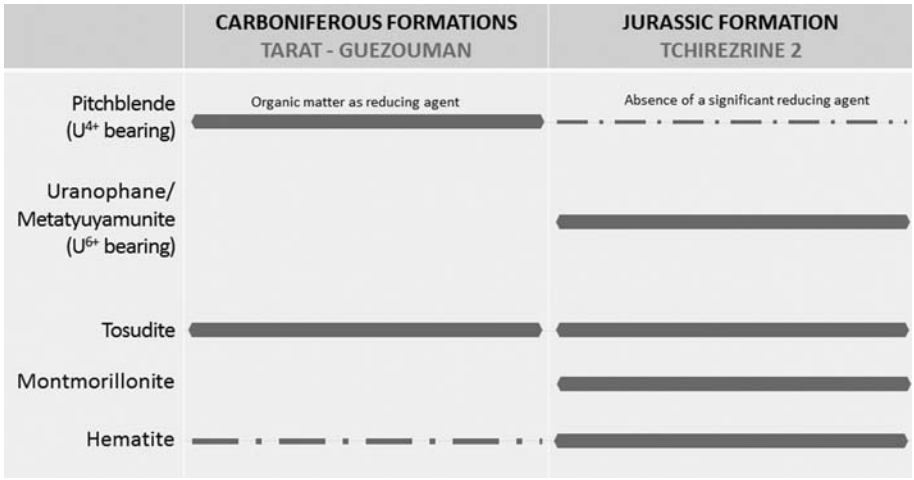

FIG. 11. Diagram of relationships between a late alteration event allowing crystallization of tosudite (and montmorillonite + hematite) and uranium-bearing mineral crystallization.

chlorites at the regional scale but in minor amounts that are difficult to identify by routine XRD analysis.

The temperature at which tosudite formed in the sandstone formations of the Tim Mersoï sub-basin is not known, but it probably ranged between 100 and 200°C according to the data given in the literature for the thermal stability of tosudite (Beaufort *et al.*, 2015). In the same chemical system, sudoite is the stable phase which replaces tosudite at temperatures of >200°C (Vidal *et al.*, 2012 and references therein). Moreover, the fact that some of the analyses of the tosuditic clay are close to the sudoite end-member in the Carboniferous formation and some of the analyses of the tosuditic clay are near to the montmorillonite end-member in the Jurassic formation (Fig. 10) is probably indicative of different temperature of crystallization; tosudite should have crystallized at temperatures near its upper limit of thermal stability in the Carboniferous sandstones (Arlit area) whereas it crystallized at temperatures near its lower limit of thermal stability in Jurassic sandstones (Imouraren area).

CONCLUSION

The main goals of this study were to characterize the crystal-chemical properties of tosudite from the Tim Mersoï basin and to identify precisely the petrogenetic relationships between this unusual clay mineral and U deposits of the Tarat, Guezouman and Tchirezrine 2 formations. This clay mineral has been shown to present all the characteristics of the diagenetic tosudite

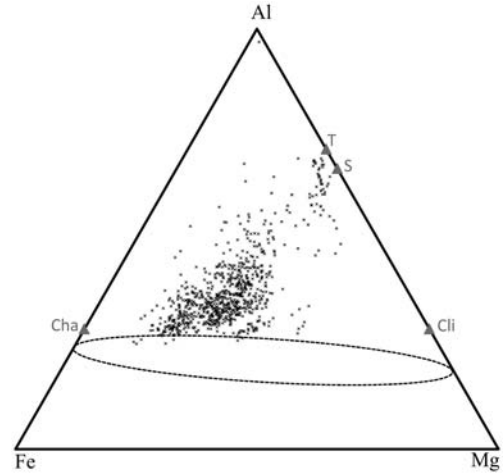

FIG. 12. Representation of WDS analyses of chlorite from Arlit and Imouraren areas in triangular diagram Al^{VI}-Fe-Mg (all Al considered as octahedral). The WDS analyses of chlorite (crosses) are from various studies (Forbes, 1986; Cavellec, 2006; Patrier *et al.*, 2009; Billon *et al.*, 2009). The dashed ellipse = composition field of common chlorites (Rigault, 2010 and references therein). Grey triangles represent pure phases: Cha, chamosite $(Si_3Al)O_{10}(Fe^{2+}_5Al)(OH)_8$; Cli, clinochlore $(Si_3Al)O_{10}(Mg_5Al)(OH)_8$; S, sudoite $(Si_3Al)O_{10}(Mg_2Al_3)(OH)_8$; T, tosudite (*i.e.* Table 1).

reported in the literature (*i.e.* it is consistent with 1:1 regular interstratification of di-trioctahedral chlorite (sudoite) and low-charge montmorillonite). However,

https://doi.org/10.1180/claymin.2016.051.4.07 Published online by Cambridge University Press

sandstone petrography is not consistent with a diagenetic origin of this mineral, which post-dates and replaces the diagenetic minerals of the reduced sandstones. The phase relationships between tosudite, uranium minerals and Fe oxides and the very small amount of Fe in tosudite allow us to relate the occurrence of tosudite to a late alteration event during which uranium was remobilized by oxidizing fluids of probable sedimentary origin. Both the origin and the age of the different stages of water–rock interaction and their relationships with the tectono-thermal history of this part of the Tim Mersoï basin are of prime importance to improving the genetic model of Nigerian uranium deposits (Pagel *et al*., 2005). Further investigations are needed into the alteration stage which has probably remobilized the uranium at a regional scale. In particular better constraints on the regional extent of tosudite are needed to decipher its spatial relationships with the Arlit fault. Another prospective work would be to conduct thermodynamic calculations of the physico-chemical conditions (particularly in terms of Eh-pH) at which tosudite crystallized in the Tim Mersoï basin.

ACKNOWLEDGEMENTS

The authors thank the AREVA mining company for funding this work through Masters internships and a PhD thesis. They are also grateful to thank Stephen Hillier, Julita Biernacka and an anonymous reviewer for reviewing an earlier version of this work.

REFERENCES

Bailey S.W. (1982) Nomenclature for regular interstratifications. *American Mineralogist*, **67**, 394–398.

Bartier D., Ledesert B., Clauer N., Meunier A., Liewig N., Morvan G. & Addad A. (2008) Hydrothermal alteration of the Soultz-sous-Forets granite (Hot Fractured Rock geothermal exchanger) into a tosudite and illite assemblage. *European Journal of Mineralogy*, **20**, 131–142.

Beaufort D., Meunier A., Patrier P. & Ottaviani M.M. (1992) Significance of the chemical variations in assemblages including epidote and/or chlorite in the fossil geothermal field of Saint Martin (Lesser Antilles). *Journal of Volcanology and Geothermal Research*, **51**, 95–114.

Beaufort D., Baronnet A., Lanson B. & Meunier A. (1997) Corrensite: a single phase or a mixed-layer phyllosilicate in the saponite-to-chlorite conversion series? A case study of Sancerre-Couy deep drill hole (France). *American Mineralogist*, **82**, 109–124.

Beaufort D., Cassagnabere A., Petit S., Lanson B., Berger G., Lacharpagne J.C. & Johansen H. (1998) Kaolinite-to-dickite reaction in sandstone reservoirs. *Clay Minerals*, **33**, 297–316.

Beaufort D., Rigault C., Billon S., Billault V., Inoue A., Inoue S. & Patrier P. (2015) Chlorite and chloritization processes through mixed-layer mineral series in low-temperature geological systems – A review. *Clay Minerals*, **50**, 497–523.

Billault V., Beaufort D., Patrier P. & Petit S. (2002) Crystal chemistry of Fe-sudoites from uranium deposits in the Athabasca basin (Saskatchewan, Canada). *Clays and Clay Minerals*, **50**, 70–81.

Billon S. (2014) *Minéraux argileux dans le gisement uranifère d'Imouraren (Bassin de Tim Mersoï, Niger): Implications sur la genèse du gisement et sur l'optimisation des processus de traitement du minerai*. Phd thesis, University of Poitiers, France, 340 pp.

Billon S., Beaufort D. & Sardini P. (2009) *Processus D'altération Dans Les Corps Gréseux (Izégouande, Tarat et Guézouman) Au Voisinage De La Faille D'Arlit (Niger)*. Unpublished Masters thesis, University of Poitiers, France, 38 pp.

Billon S., Beaufort D., Sardini P. & Wattinne A. (2013) Occurrence of Tosudite in Uranium deposits of the Arlit area (Niger). *XV International Clay Conference*, 7–11 July 2013, Rio de Janeiro, Brazil.

Bish D.L. & Reynolds R.C. Jr (1989) Sample preparation for X-ray diffraction. Pp. 73–99 in: *Modern Powder Diffraction* (D.L. Bish & J.E. Post, editors). Reviews in Mineralogy, **20**, Mineralogical Society of America, Washingon, D.C.

Brown G., Bourguignon P. & Thorez J. (1974) A lithium-bearing aluminian regular mixed layer montmorillonite-chlorite from Huy, Belgium. *Clay Minerals*, **10**, 135–144.

Cavellec S. (2006) *Evolution diagénétique du bassin de Tim Mersoï et conséquences pour la genèse des minéralisations uranifères dans les formations carbonifères du Guézouman et du Tarat (district Arlit-Akokan, Niger)*. Unpublished PhD thesis, University Paris-Sud XI, France, 428 pp.

Creach M., Meunier A. & Beaufort D. (1986) Tosudite crystallization in the kaolinitized granitic cupola of Montebras, Creuse, France. *Clay Minerals*, **21**, 225–230.

Coquel R., Lang J. & Yahaya M. (1995) Palynologie du Carbonifère du Nord Niger et de la plateforme saharienne: implications stratigraphiques et paléogéographiques. *Review of Palaeobotany and Palynology*, **89**, 319–334.

Daniels E.J. & Altaner S.P. (1990) Clay mineral authigenesis in coal and shale from the Anthracite region, Pennsylvania. *American Mineralogist*, **75**, 825–839.

Forbes P. (1989) *Rôle des structures sédimentaires et tectoniques, du volcanisme alcalin régional et des fluides diagénétiques – hydrothermaux pour la formation des minéralisations à U-Zr-Zn-V-Mo*

https://doi.org/10.1180/claymin.2016.051.4.07 Published online by Cambridge University Press

d'Akouta (Niger). Unpublished PhD thesis, University of Bourgogne, France, 375 pp.

Frank-Kamenetskii V.A., Logvinenko N.V. & Drits V.A. (1965) Tosudite – a new mineral, forming the mixed layer phase in alushtite. *Proceedings of the International Clay Conference, Stockholm*, **2**, 181–186.

Garvie L.A.J. (1992) Diagenetic tosudite from the lowermost St Maugham's Group, Lydney Harbour, Forest of Dean, UK. *Clay Minerals*, **27**, 503–513.

Gerbeaud O. (2006) *Evolution structurale du bassin de Tim Mersoï : le rôle des déformations de la couverture sédimentaire sur la mise en place des gisements uranifères du secteur d'Arlit (Niger)*. PhD thesis, University of Paris Sud, 260 pp.

Harrison M.J., Marshak S. & Onasch M. (2004) Stratigraphic control of hot fluids on anthracitization, Lackawanna synclinorium, Pennsylvania. *Tectonophysics*, **378**, 85–103.

Hillier S. (1994) Pore-lining chlorites in siliciclastic reservoir sandstones: electron microprobe, SEM and XRD data, and implications for their origin. *Clay Minerals*, **29**, 665–679.

Hillier S., Fallick A.E. & Matter A. (1996) Origin of pore-lining chlorite in the Aeolian Rotliegend of northern Germany. *Clay Minerals*, **31**, 153–171.

Hillier S., Wilson M.J. & Merriman R.J. (2006) Clay mineralogy of the Old Red Sandstone and Devonian sedimentary rocks of Wales, Scotland and England. *Clay Minerals*, **41**, 433–471.

Kulke H. (1969) Petrographie und diagenese de Stubensandsteins (mittlerer Keuper) aus Tiefbohrungen im Raum. Memmingen (Bayern). *Contributions to Mineralogy and Petrology*, **20**, 135–163.

Lanson B., Beaufort D., Berger G., Bauer A., Cassagnabère A. & Meunier A. (2002) Authigenic kaolin and illitic minerals during burial diagenesis of sandstones: a review. *Clay Minerals*, **37**, 1–22.

Merceron T., Inoue A., Bouchet A. & Meunier A. (1988) Lithium-bearing donbassite and tosudite from Echassieres, Massif Central, France. *Clays and Clay Minerals*, **36**, 39–46.

Morrison S.J. & Parry W.T. (1986) Dioctahedral corrensite from Permian red beds, Libson valley, Utah. *Clays and Clay Minerals*, **34**, 613–624.

Nelson D.O. & Guggenheim S. (1993) Inferred limitations to the oxidation of Fe in chlorite: a high-temperature single-crystal X-ray study. *American Mineralogist, 78*, 1197–1207.

Nishiyama T., Shimoda S., Shimosaka K. & Kanaoka S. (1975) Lithium-bearing tosudite. *Clays and Clay Minerals*, **23**, 337–342.

Pablo-Galan L. & Chavez-Garcia M.L. (1994) Dioctahedral tosudite in hydrothermally altered Pliocene rhyolitic tuff, Neutla, Mexico. *Clays and Clay Minerals*, **42**, 114–122.

Pacquet A. (1968) Analcimes et argiles diagénétiques dans les formations sédimentaires de la région d'Agades (République du Niger). *Mémoire Service Carte Géologique Alsace-Lorraine, France*, 27–221.

Pacquet A. (1969) *Analcimes et argiles diagénétiques dans les formations sédimentaires de la région d'Agadès (République du Niger)*. PhD thesis, University of Strasbourg, France, 258 pp.

Pagel M., Cavellec S., Forbes P., Gerbaud O., Vergely P., Wagani I. & Mathieu R. (2005) Uranium deposits in the Arlit area. Pp. 303–305 in: *Mineral Deposit Research: Meeting the Global Challenges*, Vols **1** and **2** (J. Mao and F. P. Bierlein, editors). Springer-Verlag, Berlin.

Patrier P., Billon S. & Beaufort D. (2009) *Distribution Spatiale Des Chlorites Magnésiennes et Des Chlorites Ferrifères Rencontrées Autour De La Faille d'Arlit.* Unpublished technical report, University of Poitiers, France, 48 pp.

Riegler T., Beaufort D., Wollenberg P. & Lescuyer J.L. (2014) New insight from alteration related to uranium deposits in the Kiggavik-Andrew Lake trend, Nunavut, Canada. *The Canadian Mineralogist*, **52**, 27–45.

Rigault C. (2010) *Cristallochimie du fer dans les chlorites de basse température: implications pour la géothermométrie et la détermination des paléoconditions rédox dans les gisements d'uranium*. Unpublished PhD thesis, University of Poitiers, France, 259 pp.

Sempéré T. (1981) *Le contexte sédimentaire du gisement d'uranium d'Arlit (République du Niger)*. PhD thesis, Ecole nationale supérieure des mines de Paris, 392 pp.

Shimoda S. (1969) New data for tosudite. *Clays and Clay Minerals*, **17**, 179–184.

Sudo T. & Kodama H. (1957) An aluminian mixed-layer mineral of montmorillonite-chlorite. *Zeitschrift für Kristallographie*, **109**, 379–387.

Valsardieu C. (1971) *Etude géologique et paléogéographique du bassin de Tim Mersoï, région d'Agadès (République du Niger)*. PhD thesis, University of Nice, France, 518 pp.

Velde B. (1985) *Clay Minerals: A Physical-Chemical Explanation of their Occurrence.* Elsevier, Amsterdam, 427 pp.

Wilson M.J. (1971) Clay mineralogy of the Old Red Sandstone (Devonian) of Scotland. *Journal of Sedimentary Petrology*, **41**, 995–1007.

https://doi.org/10.1180/claymin.2016.051.4.07 Published online by Cambridge University Press